

Numerical investigation of Nernst effect in quasi-one-dimensional systems

Weida Wu

Department of Physics and Astronomy, Rutgers University, Piscataway, New Jersey 08854, USA

P. M. Chaikin

Department of Physics, New York University, New York, New York 10003, USA

(Received 14 June 2007; revised manuscript received 4 August 2007; published 8 October 2007)

Recent theoretical and experimental studies show that the Lebed “magic angle” effects (for magnetic field rotations in the least conducting, y - z , plane of quasi-one-dimensional conductors) can be greatly enhanced by the presence of a field along the most conducting, x , direction. Here, we complete the picture with numerical Boltzmann calculations including the Nernst effect S_{zx} . Our results confirm that B_x enhances the σ_{zz} peaks at magic angles, but does not qualitatively affect the angular dependence of the Nernst effect S_{zx} . These results suggest that the magic angle effect cannot be explained simply by the Boltzmann transport of quasiparticles on the Fermi surface.

DOI: [10.1103/PhysRevB.76.153102](https://doi.org/10.1103/PhysRevB.76.153102)

PACS number(s): 74.70.Kn, 72.15.Gd

Quasi-one-dimensional electronic systems, such as $(\text{TMTSF})_2X$ ($X=\text{PF}_6$, ClO_4 , etc.), show rich ground states ranging from superconductor to field-induced spin-density wave insulator, depending on pressure, temperature, and magnetic field.¹ The crystal structure consists of platelike TMTSF molecules which stack with strong wave function overlap in chains (a axis). The intrachain bandwidth is ~ 1 eV, while the interchain couplings give anisotropic bandwidths of 0.1 and 0.003 eV in the approximately orthogonal directions. In the “metallic” phase under moderate magnetic field, a fascinating phenomenon, the so-called Lebed magic angle effect, was discovered^{2–4} after Lebed’s initial prediction.^{5,6} The first manifestations of the magic angle effect were sharp resistance dips when the magnetic field was aligned at interchain directions in real space (lattice vectors⁷). In reciprocal space, a field along the magic angles induces electron motion along commensurate \mathbf{k} space orbits.⁸ Despite many theoretical efforts to describe the magic angle effects,^{7–20} there is as yet no satisfactory explanation. Recently, the second manifestations of the magic angle effects, giant Nernst resonances, were discovered in $(\text{TMTSF})_2\text{PF}_6$ under pressure.^{21,22} The magnitude of the Nernst signal at 1 K is at least 3 orders of magnitude larger than what we expected from simple (Drude and/or Boltzmann) estimations. The sign change of the Nernst effect at the magic angles strongly suggests that the transport is coherent only in planes defined by the chains and the interchain direction close to the applied field. The giant Nernst resonances and giant Nernst effect have also been observed in the sister compound $(\text{TMTSF})_2\text{ClO}_4$.^{23,24} Both the sign change at the magic angles and the large magnitude of the signal are not yet explained, but the effect appears generic for these materials. Any theoretical description of the magic angle effect should explain both resistivity dips and the resonantlike Nernst effect.

In most magic angle experiments (bc rotation), a component of magnetic field along the a axis caused by misalignment is usually assumed to be small and not important. (Hereafter, we will use x , y , z and a , b , c interchangeably ignoring the slight deviation of the crystal structure from

orthorhombic.) It has been indicated in previous experiments and calculations^{9,25} that this small magnetic field component is responsible for the observed sharp and pronounced magic angle effects. This picture is confirmed by either semiclassical transport theory or (in)coherent interplane single particle tunneling.^{15,17–19} A recent 4π rotation study of the conductivity of $(\text{TMTSF})_2\text{PF}_6$ by Kang *et al.*²⁶ provides experimental support to this idea. However, none of these studies addresses whether the giant Nernst resonances found at magic angles can also be explained by introducing a finite magnetic field along the a axis. In this Brief Report, we present numerical calculations of both conductivity σ_{zz} and the Nernst effect S_{zx} to study the effect of adding a magnetic field along the a axis. Details of our calculation methods have been published in Ref. 22. The dispersion relation we use in these calculations is

$$\varepsilon(\mathbf{k}) = -2t_a \cos(k_x a) - 2t_b \cos(k_y b) - 2t_c \cos(k_z c). \quad (1)$$

The band is $3/4$ filled. The numerical calculations involve an integration procedure after solving semiclassical equations of motion, while the analytic results are from an analytic approximation to the band structure [Eq. (1)] using linear dispersion along a plus first order correction to account for the nonlinear dispersion along a .²² It is worth noting that a system with linear energy dispersion has neither Hall effect nor thermoelectric effects. Therefore, it is crucial to include the nonlinear correction, which is ignored in most previous analytic studies, for calculating the Nernst effect. Our results agree with previous numerical calculations²⁰ and the analytic results^{15,17–19} by showing the enhancement of the c -axis conductivity at magic angles with a strong magnetic field along the a axis. However, qualitatively, the Nernst effect is not affected by putting even a very large magnetic field along the a axis. Therefore, we conclude that the large Nernst resonance in the magic angle effect cannot be explained by the Boltzmann transport of noninteracting particles on a quasi-one-dimensional Fermi surface.

Figure 1 shows the calculated and measured conductivity in the least conducting c direction. We see in (a) that the conductivity peaks (i.e., resistivity dips) at magic angles (la-

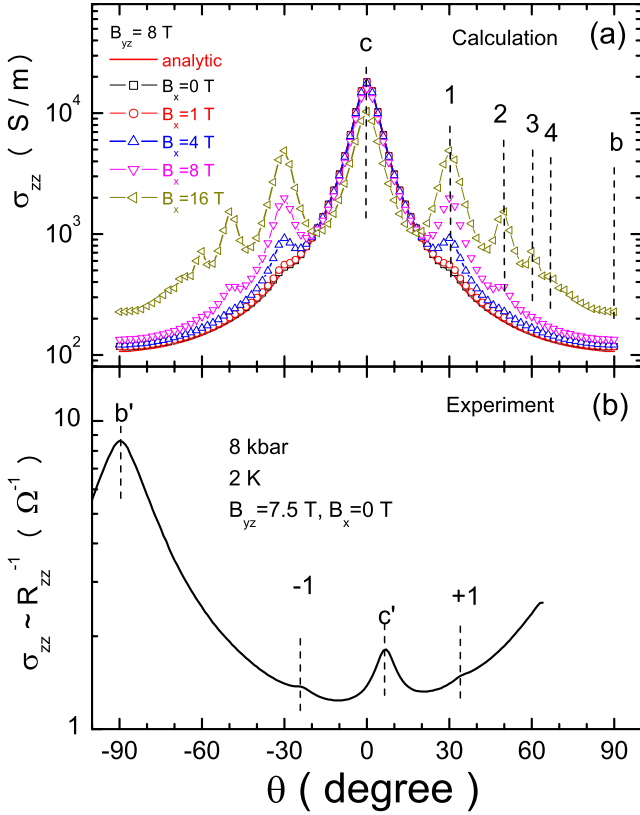


FIG. 1. (Color online) (a) Boltzmann calculation of the conductivity σ_{zz} along the least conduction axis (c axis). We fix the magnetic field component along the a axis (0, 1, 4, 8, and 16 T), while rotating the magnetic field component ($B_{yz}=8$ T) in the b - c plane. The analytic result is calculated with $B_x=0$ T. (b) Experimental data of $\sigma_{zz} \propto R_{zz}^{-1}$ of a (TMTSF) $_2$ PF $_6$ sample measured at 8 kbar, 2 K with $B_{yz}=7.5$ T, $B_x=0$ T. Note that the conductivity peak at b' cannot be explained by the calculation.

beled by 1, 2, 3, and 4) become pronounced as we increase the magnetic field component along the a axis. We can gain some insight into the origin of magnetoresistance from the following arguments. In the presence of magnetic field, electrons traverse the Fermi surface and effectively average the v_c along their orbits. If an electron orbit samples v_c symmetrically and uniformly, then $\langle v_c \rangle = 0$ and the result is a magnetoresistance which increases quadratically in the applied field without saturation. For the dispersion relation in Eq. (1), the orbits yield $\langle v_c \rangle = 0$ for any field orientation in the b - c plane except $\mathbf{B} \parallel c$ and to a lesser extent $\mathbf{B} \parallel c+b$. Thus, there should be conductivity peaks or resistivity dips at these angles. However, if we apply a field in the a direction as well, the symmetric periodic orbits at the magic angles $\mathbf{B} \parallel c+nb$ become asymmetric and no longer average to zero.¹⁵ The fact that we indeed find an enhanced magic angle effect in conductivity as the component of \mathbf{B} along a is increased demonstrates that our numerical calculation is reliable within this semiclassical model.²⁰

It has been proposed that the nonsymmetric orbits might be the reason that experimentally observed magic angle dips are sharper and more pronounced than those by Boltzmann calculations with reasonable band parameters and relaxation

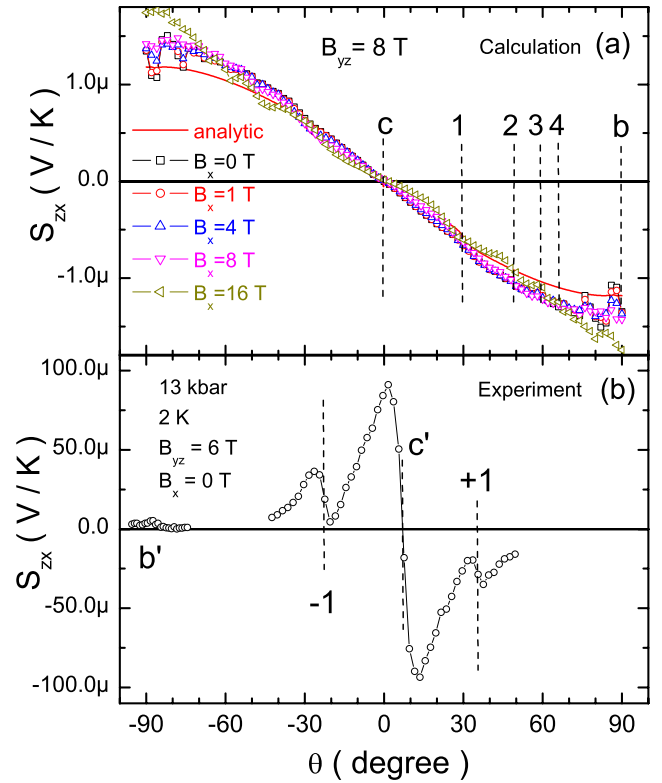


FIG. 2. (Color online) Comparison of angular dependence of the Nernst effect S_{zx} between Boltzmann calculations and experimental data. (a) Boltzmann calculation of the Nernst effect S_{zx} . We fix the magnetic field component along the a axis (0, 1, 4, 8, and 16 T), while rotating the magnetic field component ($B_{yz}=8$ T) in the b - c plane. The analytic result is calculated with $B_x=0$ T. (b) Experimental data of the Nernst effect S_{zx} of a (TMTSF) $_2$ PF $_6$ sample measured at 13 kbar, 2 K with $B_{yz}=6.0$ T.

times.^{8,20,26} Often, the alignment of the crystal with respect to external magnetic field is done by the experimenter's eyes through a microscope. A few degrees of error are usually unavoidable. The misalignment could be worse for (TMTSF) $_2$ PF $_6$ under pressure because the sample position might vary during pressurization of the pressure cell. It is worth noting that significantly large B_x (and/or B_{yz}) is still needed to obtain sharp resistivity dips at magic angles with realistic parameters [Fig. 1(a)].

If the magnetoresistance is a simple single particle transport effect aided by the field along a , then it should be able to explain the giant Nernst resonances at magic angles.²¹⁻²³ It has been shown that the Boltzmann transport fails to explain the resonantlike Nernst effect at magic angles and their giant magnitude, when there is no magnetic field component along the a axis [$B_x=0$ curve in Fig. 2(a)].²² Clearly, the giant resonantlike Nernst signal found in experiment [Fig. 2(b)] cannot be explained without a field along a . On the other hand, it is hard to guess whether the Nernst resonances can be enhanced by adding magnetic field component along the a axis, as seen in σ_{zz} [Fig. 1(a)]. This motivated us to perform numerical studies on the Nernst effect with B_x .²⁸

As shown in Fig. 2(a), qualitatively, there is no significant change of the Nernst effect S_{zx} caused by adding a magnetic

field component along the a axis. This is in sharp contrast to the conductivity σ_{zz} [Fig. 1(a)], where $B_x=4$ T is enough to produce significant enhancement at magic angles. We have tried several grid spacings and/or longer integration cut-off limits and found that they do not change the results significantly. Therefore, we conclude that neither the giant value nor the resonant like shape of the Nernst effect at magic

angles can be reproduced by the Boltzmann transport of quasiparticles on quasi-one-dimensional Fermi surfaces, even with a strong magnetic field component along the conduction chain direction. In order to understand the magic angle effect, one has to go beyond the single particle picture by including correlations in these quasi-one-dimensional systems.

-
- ¹T. Ishiguro, K. Yamaji, and G. Saito, *Organic Superconductor* (Springer, New York, 1997).
- ²T. Osada, A. Kawasumi, S. Kagoshima, N. Miura, and G. Saito, *Phys. Rev. Lett.* **66**, 1525 (1991).
- ³M. J. Naughton, O. H. Chung, M. Chaparala, X. Bu, and P. Coppers, *Phys. Rev. Lett.* **67**, 3712 (1991).
- ⁴W. Kang, S. T. Hannahs, and P. M. Chaikin, *Phys. Rev. Lett.* **69**, 2827 (1992).
- ⁵A. G. Lebed, *Pis'ma Zh. Eksp. Teor. Fiz.* **43**, 137 (1986) [*JETP Lett.* **43**, 174 (1986)].
- ⁶A. G. Lebed and P. Bak, *Phys. Rev. Lett.* **63**, 1315 (1989).
- ⁷S. P. Strong, D. G. Clarke, and P. W. Anderson, *Phys. Rev. Lett.* **73**, 1007 (1994).
- ⁸T. Osada, S. Kagoshima, and N. Miura, *Phys. Rev. B* **46**, 1812 (1992).
- ⁹T. Osada, *Physica B* **256-258**, 633 (1998).
- ¹⁰K. Maki, *Phys. Rev. B* **45**, 5111 (1992).
- ¹¹V. M. Yakovenko, *Phys. Rev. Lett.* **68**, 3607 (1992).
- ¹²P. M. Chaikin, *Phys. Rev. Lett.* **69**, 2831 (1992).
- ¹³A. G. Lebed, *J. Phys. I* **6**, 1819 (1996).
- ¹⁴N. P. Ong, W. Wu, P. M. Chaikin, and P. W. Anderson, *Europhys. Lett.* **66**, 579 (2004).
- ¹⁵A. G. Lebed and M. J. Naughton, *Phys. Rev. Lett.* **91**, 187003 (2003).
- ¹⁶A. G. Lebed, N. N. Bagmet, and M. J. Naughton, *Phys. Rev. Lett.* **93**, 157006 (2004).
- ¹⁷T. Osada, *Physica E (Amsterdam)* **12**, 272 (2002).
- ¹⁸B. K. Cooper and V. M. Yakovenko, *Phys. Rev. Lett.* **96**, 037001 (2006).
- ¹⁹U. Lundin and R. H. McKenzie, *Phys. Rev. B* **70**, 235122 (2004).
- ²⁰T. Osada, N. Kami, R. Kondo, and S. Kagoshima, *Synth. Met.* **103**, 2024 (1999).
- ²¹W. Wu, I. J. Lee, and P. M. Chaikin, *Phys. Rev. Lett.* **91**, 056601 (2003).
- ²²W. Wu, N. P. Ong, and P. M. Chaikin, *Phys. Rev. B* **72**, 235116 (2005).
- ²³E. S. Choi, J. S. Brooks, H. Kang, Y. J. Jo, and W. Kang, *Phys. Rev. Lett.* **95**, 187001 (2005).
- ²⁴M.-S. Nam, A. Ardavan, W. Wu, and P. M. Chaikin, *Phys. Rev. B* **74**, 073105 (2006).
- ²⁵I. J. Lee and M. J. Naughton, *Phys. Rev. B* **57**, 7423 (1998).
- ²⁶W. Kang, T. Osada, Y. J. Jo, and H. Kang, *Phys. Rev. Lett.* **99**, 017002 (2007).
- ²⁷G. M. Danner, W. Kang, and P. M. Chaikin, *Phys. Rev. Lett.* **72**, 3714 (1994).
- ²⁸Briefly, we use the band parameters ($t_a=0.25$ eV, $t_b=0.024$ eV, and $t_c=0.0008$ eV) from tight binding approximations, realistic lattice parameters ($a=3.49$ Å, $b=7.7$ Å, and $c=13.264$ Å), and a scattering time $\tau=4.26 \times 10^{-12}$ s from previous studies by Danner *et al.* (Ref. 27). The integration cut-off limit is 20τ . Here, we use $B_{yz}=8$ T, and $T=1$ K, which are comparable with experiment conditions. We use either 10×10 or 20×20 (for $B_x > 8$ T) grids on the Fermi surface in the calculations.